Nucleation and growth of aluminum on an inert substrate of graphite

2008 J. Phys.: Condens. Matter 20 225002

(http://iopscience.iop.org/0953-8984/20/22/225002)

IOP PUBLISHING JOURNAL OF PHYSICS: CONDENSED MATTER

J. Phys.: Condens. Matter **20** (2008) 225002 (6pp) doi:10.1088/0953-8984/20/22/225002

Nucleation and growth of aluminum on an inert substrate of graphite

Wende Xiao[1,2,3], Sunil Singh Kushvaha[1] and Xue-sen Wang[1]

[1] Department of Physics and NUS Nanoscience and Nanotechnology Initiative, National University of Singapore, 2 Science Drive 3, 117542, Singapore
[2] Beijing National Laboratory for Condensed Matter Physics, Institute of Physics, Chinese Academy of Sciences, PO Box 603, Beijing 100080, People's Republic of China

E-mail: wdxiao@aphy.iphy.ac.cn

Received 22 January 2008, in final form 18 March 2008
Published 16 April 2008
Online at stacks.iop.org/JPhysCM/20/225002

Abstract

We have investigated the nucleation, growth and structure of Al on an inert graphite surface at room temperature (RT) using *in situ* scanning tunneling microscopy. It was observed that Al initially nucleates at step edges and defect sites of graphite surfaces, due to the inertness of the substrate and weak interfacial interaction. From a diffusion and capture model, the mean adatom diffusion length before desorption was derived to be 170 ± 80 nm, correspondingly giving a lower bound of the adatom–substrate binding energy of 0.39 ± 0.03 eV. With successive Al deposition of ~0.5 nm, the growth and coarsening of small clusters results in flat-top crystalline islands with (111)-oriented facets located at step edges as well as on defect-free terraces. The crystalline islands have essential translational and rotational mobility, which leads to the formation of craters on islands after Al deposition of ~6 nm. A simple island-coalescence model based on fast edge diffusion and suppressed detachment from step edges was proposed for rationalizing the crater formation. It was also observed that isolated islands of Al can be stabilized by two-dimensional structures of Sb surrounding Al islands after Sb deposition at RT.

1. Introduction

The morphology and structure of a growing surface is ultimately governed by the bonding and motion of individual atoms on surfaces [1, 2]. Growth is the integrated effect of a variety of elemental processes of individual atoms characterized by delicate energy parameters for bonding and diffusion. In conventional island nucleation theory of single-atom deposition, stable islands consisting of two or more atoms are assumed to be immobile due to a strong adatom–surface interaction [1–3]. The islands grow by capturing single atoms which diffuse across the surface. Islands can be varied from fractal or ramified (or dendritic) to compact shape, depending on different energy barriers for various diffusions, e.g. single-atom migration on terraces, along island edges and across corners [1, 2]. The top surfaces of islands are usually flat or protruding because of the asymmetry of step barrier, namely, a lower barrier for diffusion downwards than upwards.

However, the scenario of growth becomes different when the substrate is chemically inert. In this case, the adatom–surface interaction is very weak, leading to low diffusion barriers for single atoms as well as clusters. Thus both single atoms and clusters with size smaller than a critical value can migrate on the surfaces with remarkable rates. Initial nucleation only occurs at step edges and defect sites, because a relatively strong interaction there can stabilize nuclei. The morphologies of islands are also affected by the mobility of clusters. The island shapes are determined by the competition between two typical times: (1) the coalescence time of a cluster and an island; and (2) the collision interval time between the arrivals of clusters on the same island. This behavior is, in some degree, similar to the growth of cluster deposition [4, 5], whereas it is very different from the case with a strong adatom–surface interaction, in which only single-atom processes occur and it is not necessary to consider the mobility of clusters and islands [1, 2]. Therefore, islands with unique shapes and structures can be prepared on inert substrates by the adjustment of growth parameters (e.g. substrate temperature

[3] Author to whom any correspondence should be addressed.

and deposition flux), which may exhibit unique properties and have potential applications.

As a chemically inert conductor, graphite is a good prototypical substrate for exploration of the growth and structure of nanostructures on an inert surface, and has attracted significant interest in recent years, due to potential applications in microelectronics, optoelectronics and catalysis [6]. Al being a simple metal with a face-center cubic (fcc) structure, its growth, interfacial reaction and local atomic arrangement on graphite have been studied extensively in recent years [7–14]. Experimental and theoretical investigations indicate a very weak adatom–substrate interaction [10, 11]. But most of them are focused on adatoms or small clusters of Al on graphite [7–9, 12]. Possibly due to different preparation methods for Al clusters or *ex situ* characterization processes, there are some contradictory descriptions as regards the nucleation and growth of Al on graphite. The structure and stability of large islands with a size of several hundred nanometers have not been well explored yet.

In this work, we report an *in situ* investigation of the nucleation, growth, structure and mobility of Al islands on highly oriented pyrolytic graphite (HOPG) surfaces at room temperature (RT) using scanning tunneling microscopy (STM). We observe preferential nucleation at step edges and the formation of (111)-oriented islands with hexagonal craters, due to remarkable mobility of both individual adatoms and clusters of Al on the surfaces, which originates from the inertness of the graphite substrates. We also found that the isolated islands of Al can be stabilized by two-dimensional (2D) structures of Sb surrounding Al islands after Sb deposition at RT.

2. Experiments

The experiments were conducted in an ultrahigh vacuum (UHV) system (base pressure $<1 \times 10^{-10}$ mbar) equipped with STM and a four-grid optics for low energy electron diffraction (LEED) and Auger electron spectroscopy (AES). After cleaving in the atmosphere, the HOPG substrate was transferred into the UHV chamber immediately and degassed at ∼500 °C for more than 10 h before use. The Al doser consisted of an Al wetted W filament. Sb was evaporated from a W boat. The evaporation rates were controlled by the currents through the W filament and boat. Both sources were thoroughly degassed before evaporation. During any evaporation, the chamber pressure remained below 3×10^{-10} mbar. At typical operating temperature of ∼400 °C, Sb mostly evaporates as Sb_4 [15]. The fluxes were calibrated by AES and STM. As Al grows on graphite in a three-dimensional (3D) island mode, we use the nanometer (nm) as the measurement of the Al coverage, where 1 nm corresponds to 4.3 layers of close-packing Al in bulk. All STM images were taken in constant current mode at RT.

3. Results and discussion

3.1. Nucleation at step edges and defect sites

Figure 1 shows an STM image of HOPG with ∼0.3 nm Al deposited at RT. It is obvious that chains of Al clusters

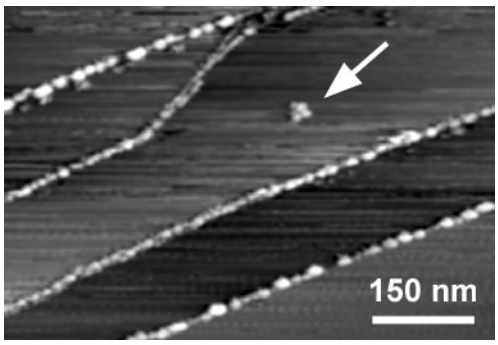

Figure 1. STM image showing 3D spherical Al clusters and cluster chains at steps and defect sites after Al deposition of ∼0.3 nm at RT. The arrow indicates three clusters located at a defect site on the terrace ($V_s = 0.4$ V, $I_t = 0.3$ nA).

form along the step edges at the early stage. A group consisting of three small clusters (indicated by an arrow) can be seen on a terrace, possibly located at a defect site. This nucleation behavior is consistent with previous theoretical and experimental investigations showing that the interfacial reaction between Al and HOPG is too weak to stabilize planar epitaxial structures at RT in the absence of defects, and initial nucleation only occurs at step edges and defect sites [13, 14]. Similar observations were also reported on the growth of Ag and Au on HOPG [16–19]. We note that most small clusters are nearly spherical, whereas some large clusters have oval and dumbbell shapes, indicating a migration and coalescence of clusters [16]. These 3D clusters have an apparent height in the range of 3–6 nm with respect to the HOPG surface.

The preferential nucleation at step edges is well known and an atomistic model was proposed by Gates and Robins [20]. In this model, atoms deposited on the substrate diffuse randomly until they either arrive at step edges or re-evaporate from the surface. Once an atom is captured by a step edge, it will randomly migrate along the step edge without leaving, as a stronger binding presents at step edges than at defect-free terraces. Collision of two atoms diffusing along a step edge leads to the formation of a critical nucleus, which is assumed to be immobile. This nucleus then grows by collecting other adatoms, and finally cluster chains form along the step edges. If the steps are sufficiently close together and the substrate temperature is high enough that there is no competitive capture of adatoms by nuclei on defect-free terraces, then the total rate of arrival of adatoms at a step edge from both sides is independent of time and has the form

$$J = FW = F\lambda[\tanh(d_1/2\lambda) + \tanh(d_2/2\lambda)] \qquad (1)$$

where F is the effective flux of deposition of atoms onto the substrate, W represents the effective collection width of the step edge, d_1 and d_2 are the distances to the adjacent steps, and λ is the root mean square diffusion distance of an adatom on terraces before desorption. The one-dimensional density of nuclei along the step edges was also given by Gates and Robins [20]. However, as many aspects, e.g. the mobility of clusters on terraces as well as along step edges and cluster coalescence, have not been considered in this model [16], the

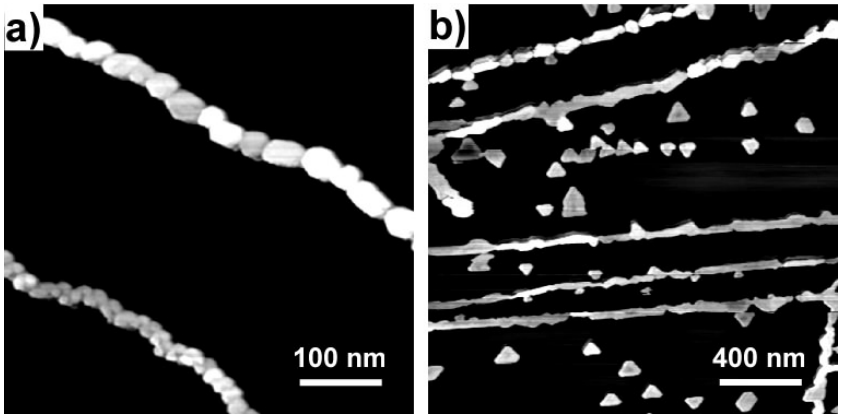

Figure 2. (a) Flat-top islands at steps after Al deposition of ∼0.5 nm at RT ($V_s = 0.5$ V, $I_t = 0.4$ nA); and (b) formation of isolated islands in defect-free areas and elongated islands at step edges after Al deposition of ∼4 nm at RT ($V_s = 3.9$ V, $I_t = 0.3$ nA).

expression for the density of nuclei may not fit our current case of Al growth on HOPG. Nevertheless, equation (1) is still a good description of the rate of arrival of adatoms at step edges, except that a cluster is viewed as a group of adatoms. The ratio of atom density along two step edges (step edge i and j) is then given by

$$R_{ij} = \frac{V_i}{V_j} = \frac{J_i}{J_j} = \frac{\tanh(d_{i1}/2\lambda) + \tanh(d_{i2}/2\lambda)}{\tanh(d_{j1}/2\lambda) + \tanh(d_{j2}/2\lambda)} \quad (2)$$

where V refers to the total volume of clusters along unit-length step edge. As V and d can be measured from STM images, λ is easily derived from equation (2). In the present case of Al growth on HOPG at RT, we get $\lambda = 170 \pm 80$ nm.

On the other hand, λ is related to the atomic energies for adsorption E_a, surface diffusion E_d, and substrate temperature T, by

$$\lambda = \frac{a}{2}\sqrt{\frac{v_d}{v_a}} \exp\left\{\frac{E_a - E_d}{2k_B T}\right\} \quad (3)$$

where a is the single hop distance ($a = 2.46$ Å for graphite), k_B is the Boltzmann constant, and v_a and v_d are the attempt frequencies for desorption and diffusion, respectively. Although v_d is expected to be a little smaller than v_a, here we approximate their ratio as unity. Taking $\lambda = 170 \pm 80$ nm in equation (3), $E_a - E_d$ is calculated to be 0.37 ± 0.03 eV. Thus a binding energy of $E_a = 0.39 \pm 0.03$ eV is obtained by using a diffusion barrier of $E_d = 0.02$ eV as calculated by Moullet [14]. Our result ($E_a = 0.39 \pm 0.03$ eV) is significantly lower than the previous experimental value of 0.8 eV proposed by Ganz *et al* and the theoretical value of 0.9 eV given by Moullet [9, 14]. We note that Ganz *et al* estimated the binding energy from the time of stay of Al monomers on HOPG during STM scanning [9]. The monomers that they observed were possibly located at defect sites due to a much stronger adatom–substrate interaction at defect sites than at the defect-free terrace. Thus their result of 0.8 eV is somewhat overestimated, and can be considered as an upper bound of E_a. On the other hand, the possible multiple hops are ignored, and a mobile cluster is treated as a group of non-interacting monomers in our model and calculations. Moullet pointed out that the binding energy per Al atom for clusters is less than the value of atomic adsorption [14]. For instance, a binding energy of 0.08 eV per Al–C bond was calculated for clusters consisting of 5–6 Al atoms [14]. Therefore, our result of ∼0.39 eV is a little underestimated for atomic adsorption, and can be viewed as a lower bound of E_a. The binding energy of 0.39–0.8 eV clearly confirms a weak adatom–substrate interaction, compared with the Al–Al binding energy (cohesive energy of 3.42 eV) [21].

3.2. Mobility of crystalline islands

After further deposition of ∼0.5 nm, Al islands still locate at the step edges exclusively, as shown in figure 2(a). Flat tops and straight edges of the islands indicate a crystalline structure. The height of the islands is in the range of about 3–5.5 nm and the planar size is about 15–25 nm, related to the width of terraces. These islands can be stably imaged when a sample bias (V_s) of 0.5 V is used. After Al deposition of ∼4 nm and with a high bias of $V_s = 3.9$ V, isolated islands nucleated and grown on terraces can be stably imaged without tip-induced movement, as shown in figure 2(b). However, when the bias is reduced to 0.5 V, isolated islands with even quite large lateral size (∼200 nm after successive Al deposition of ∼6 nm) can be dragged along on terraces by the STM tip, revealing a rather weak binding with graphite. When the isolated islands are dragged to step edges, they will stay there. Similar behaviors were also observed in the case of Au growth on HOPG [18]. This is reasonable as we know that the distance between the tip and sample reduces with decreasing bias in the constant current mode of STM scanning, leading to an increase of tip–sample interaction.

As seen in figure 2(b), most isolated islands have a truncated triangular shape, indicating a top facet of Al(111). Those with irregular shapes are probably due to island coalescence. As most isolated triangular islands show about 30° off from nearby HOPG cleavage steps, a preferential alignment with Al(111) ∥ HOPG(0001) and Al⟨110⟩ ∥ HOPG⟨10$\bar{1}$0⟩ is proposed, according to previous investigations [10, 12]. Similar atomic arrangement was also reported for Pd and Au growth on HOPG [22–24]. We note that deviations from the exact azimuthal orientation by a few degrees are not scarce, also indicating a weak interaction

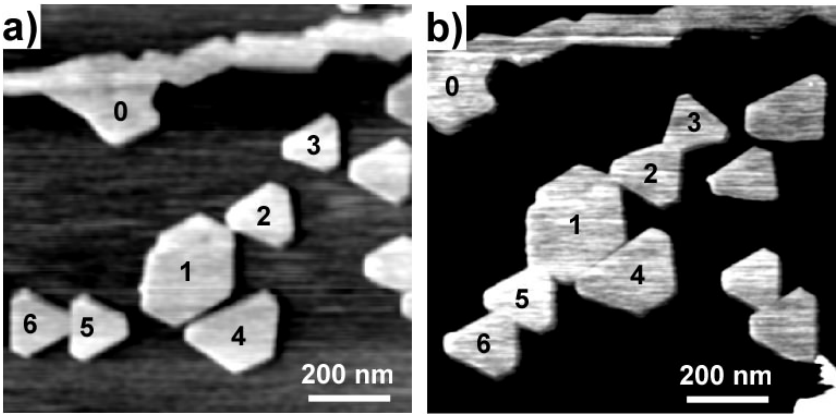

Figure 3. Consecutive STM images taken from a sample after Al deposition of ∼4 nm at RT showing island migration and rotation ($V_s = 4.6$ V, $I_t = 0.3$ nA).

between such large Al islands and graphite, so that the Al islands are indeed taking a nearly free-standing state.

Due to the weak interaction with HOPG, we find that Al islands have remarkable translational and rotational mobility. Figure 3 displays consecutive STM images showing the migration and rotation of several islands. $V_s = 4.6$ V is applied in STM scans to reduce the tip disturbance to the islands. The islands labeled '1' and '0' (near a step) are immobile (both rotational and translational) during the scan period, so they are used as references. Island '4' rotates only ∼7° and moves a short distance to get to contact and align with '1'. Island '3', however, rotates 60° and migrates ∼90 nm from its initial position to merge with '2'. Islands '5' and '6' also rotate 60° and migrate ∼100 nm from their initial positions to attach to island '1'. These dramatic rotations and translations may consist of many small steps. Previously, Anton and Kreutzer observed the displacement and rotation of gold islands on HOPG by transmission electron microscopy [24]. They attributed this mobility to electron beam-induced excitation of gold islands. In their investigation, the gold islands had a planar size of ∼20 nm and a height of ∼5 nm. The distance of island migration was a few nanometers and the angle of rotation for each step was much smaller than 10°. In the present case of Al growth on HOPG, however, the Al islands are about ten times bigger than the gold islands. The distance of Al island migration and the angle of rotation are also much greater than those of gold. Furthermore, no high energy electron beam is illuminated on the sample during our STM scanning, so the electron beam-induced mobility of Al islands can be excluded. On the other hand, supposing that the mobility of Al islands is due to the tip–island interaction, the direction and intensity of island movement should somehow follow the scan directions, which is not observed in our experiments with $V_s = 4.6$ V. Actually, we do find that when the scan bias is reduced to ∼0.5 V, a tip-induced movement of Al islands becomes very common, as the curved-belt-like traces of the moving islands can be clearly seen (not shown). Therefore, we conclude that the observed migration and rotation with $V_s = 4.6$ V are probably intrinsic properties of Al islands on HOPG. The disturbance of the tip is too weak to play a major role. In fact, it had been demonstrated that antimony and gold clusters migrate on HOPG surfaces at a surprisingly high diffusion rate of $\sim 10^{-8}$ cm^2 s^{-1} at RT [25, 26], quite comparable to that of single atoms in similar conditions. Silver clusters with a diameter of ∼14 nm were also found to be mobile on graphite surface [27]. The behavior of Al clusters on HOPG surfaces seems similar to those of Au and Ag. However, the microscopic mechanisms of island migration and rotation are still an open question.

3.3. Formation of craters on Al islands

After Al deposition of ∼6 nm, craters are observed after zoom-in on the top facets of Al islands, as shown in figures 4(a) and (b). One island may have several craters. For instance, crater chains are observed on the elongated islands at step edges. The observation of rounded hexagons of the craters also confirms that the top facets of Al islands have an Al(111) structure. The measured average height of monatomic steps is consistent with that of Al(111) in bulk phase.

The formation of 3D islands with craters on top is a very unique growth behavior and has seldom been reported before. On the basis of thermodynamic arguments, the typical Volmer–Weber or 3D growth of thin films with single-atom deposition results in islands with flat or protruding top surfaces [1, 3]. In most kinetic theories, island growth, coalescence and decay are related to single-atom diffusion, attachment or detachment processes [1, 2]. However, islands with craters have a concave curvature in our experiments, revealing a different mechanism for island formation.

Here a simple model is proposed for the mechanism of crater formation. At the initial stage, Al atoms diffuse fast on HOPG surfaces due to a low diffusion energy barrier (∼0.02 eV) [14], and the nucleation of small clusters occurs when Al atoms meet together. With further deposition of Al, small clusters grow up during diffusion due to an increasing density of Al atoms on HOPG surfaces. The grown islands gradually become immobile, while small islands still have essential mobility on defect-free areas. When several islands meet, they merge into a large coherent island. In such a coarsening process, Al atoms are required to fill in the bare HOPG surface area surrounded in the middle

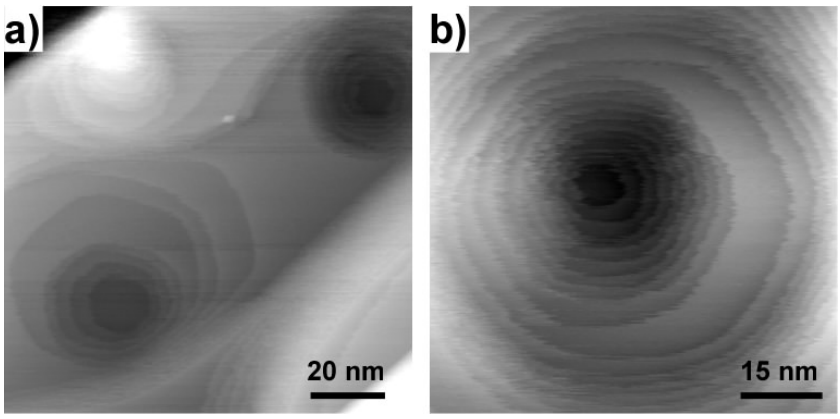

Figure 4. (a) Crater chains on elongated islands at steps ($V_s = 0.6$ V, $I_t = 0.7$ nA); and (b) craters on isolated islands dragged to step edges by the tip ($V_s = 0.6$ V, $I_t = 0.7$ nA).

of the island group. Previous investigations have shown that coalescence occurs at RT for Al islands, and kink and corner breaking induce a transition towards equilibrium-shaped islands [28–30]. However, although the energy barrier for an Al atom to jump down a step is small (0.06–0.08 eV) [30], the inter-layer mass transport is inefficient at RT due to a high energy barrier (∼0.8 eV) for atom evaporation from the steps [28]. Therefore, Al atom transport to the middle of the island group is much slower than the merging diffusion along the perimeter, leading to the formation of craters with rounded hexagonal shape in the central area of the final Al island at RT. To form a crater in the center, the minimum number of islands in the group is 3. A similar process occurs in the formation of crater chains on the elongated islands along step edges. It is noteworthy that figure 3 has actually displayed the processes for the possible formation of craters. It is seen that after the position and orientation adjustments, the lattices of islands numbers '1', '2' and '4' fit very well and it is possible for them to further evolve into an integral island with a crater in the center.

After annealing the sample shown in figure 4 at ∼350 °C for 25 min, the top facets of Al islands originally with craters are smoothed. This is due to the activation of edge evaporation at high temperature [28], leading to an enhanced inter-layer mass transport of Al islands, which further confirms our island-coalescence model for the crater formation based on fast edge diffusion and suppressed detachment from step edges.

The formation of Al islands with craters on HOPG surfaces is, in fact, a good example of unique growth behaviors on inert substrates, where both atoms and clusters have essential mobility. We believe that, depending on the competition between single-atom processes and cluster processes, the structures synthesized on inert substrates can be varied from those of single-atom deposition to those of cluster deposition by adjustment of substrate temperature, surface defects, flux, etc.

3.4. Stabilizing Al islands with Sb

Above, we have shown that the inertness of HOPG substrate offers great advantages for preparation of unique nanostructures, which are nearly free standing on the substrate. However, the interaction between the nanostructures and HOPG substrate is too weak to stabilize the nanostructures in some cases, leading to a remarkable mobility and difficulty of characterization. It is still a challenge to stabilize these nanostructures on HOPG in a simple way.

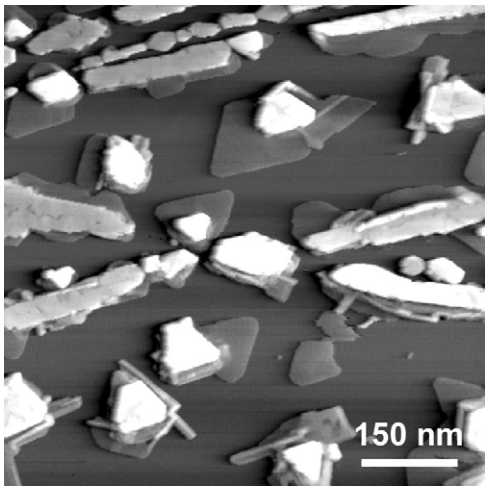

Figure 5. STM image showing that Al islands are stabilized on HOPG after Sb deposition of ∼10 nm at a flux of about 2 nm min^{-1} and at RT ($V_s = 0.6$ V, $I_t = 0.7$ nA).

Here, we introduce Sb to immobilize Al nanostructures on HOPG. Figure 5 displays STM images taken from the sample shown in figure 4 after annealing at ∼350 °C for 25 min and Sb deposition of ∼10 nm at a flux of ∼2 nm min^{-1} and at RT. As a low sample bias of 0.4 V is applied for scanning, a tip-induced movement of isolated Al islands is expected, which, however, is not observed in figure 5. Instead, the isolated islands hold their position without any displacement during scanning. Each island is surrounded by a 2D Sb structure. The white traces are attributed to small 3D clusters of Sb, which were reported to have a very high mobility on HOPG surfaces at RT [25]. Close-ups of these 2D Sb structures surrounding Al islands reveal monatomic steps with an average height of 3.85 ± 0.35 Å and a hexagonal ordered structure with a period of 4.22 ± 0.16 Å.

Within experimental uncertainty, our measured step height and lateral period are consistent with the lattice parameters of α-Sb(0001) in the rhombohedral phase [31], similar to the 2D structures of Sb growth on HOPG [32, 33]. The top facets of Al islands are covered by Sb films consisting of amorphous and 2D crystalline structures.

In previous work, we reported the preferential formation of 2D structures of Sb on HOPG at high flux, due to a conversion of physisorbed Sb_4 to chemisorption or dissociation to Sb_2 on HOPG [32, 33]. In the current case of Al on HOPG, the boundaries of Al islands serve as active sites for nucleation and growth of 2D structures of Sb surrounding Al islands. The formation of epitaxial 2D Sb structure on HOPG reveals a strong Sb–substrate interaction, leading to the stabilization of Al islands on HOPG. Therefore, the 2D Sb structures can be considered as an adhesive. As we know that a variety of metals and semiconductor nanostructures prepared on HOPG surfaces have remarkable mobility due to a weak interfacial reaction, our method might be a promising solution.

4. Conclusion

In summary, we have investigated the nucleation, growth and structure of Al on HOPG at RT using STM. The preferential nucleation and growth of Al at steps and defect sites of HOPG is analyzed with a diffusion and capture model. A mean adatom diffusion length of 170 $\pm$ 80 nm before desorption is calculated, correspondingly giving a lower bound of the adatom–substrate binding energy of 0.39 $\pm$ 0.03 eV. With successive Al deposition, (111)-oriented crystalline islands develop on terraces as well as at step edges. The islands on terraces have significant mobility in migration and rotation even with a lateral size of several hundred nanometers. The formation of hexagonal craters on Al islands is rationalized with an island-coalescence model based on fast edge diffusion and depressed detachment from step edges. Craters are found smoothed by annealing at $\sim$350 °C because of the activation of edge evaporation. It is also observed that isolated islands of Al are stabilized after Sb deposition of 10 nm at RT, due to 2D structure of Sb surrounding Al islands. A similar stabilizing effect of Sb upon other materials on HOPG is expected. Our results demonstrate that the growth of Al on graphite is a complicated process involving mobile adatoms and clusters, due to the inertness of the substrate, which clearly has implications in preparing unique nanostructures on inert substrates by controlling growth parameters.

Acknowledgments

This work was partially supported by research grants from the National University of Singapore (Grant R-398-000-008-112) and the Science and Engineering Research Council of Singapore (Grant R-144-000-088-305).

References

[1] Brune H 1998 *Surf. Sci. Rep.* **31** 121
[2] Zhang Z and Lagally M G 1997 *Science* **276** 377
[3] Venables J A, Spiller G D T and Hanbücken M 1984 *Rep. Prog. Phys.* **47** 399
[4] Jensen P 1999 *Rev. Mod. Phys.* **71** 1695
[5] Yoon B, Akulin V M, Cahuzac Ph, Carlier F, de Frutos M, Masson A, Mory C, Colliex C and Bréchignac C 1999 *Surf. Sci.* **443** 76
[6] Binns C, Baker S H, Demangeat C and Parlebas J C 1999 *Surf. Sci. Rep.* **34** 105
[7] Ganz E, Sattler K and Clarke J 1988 *J. Vac. Sci. Technol.* A **6** 419
[8] Fan W C, Strozier J and Ignatiev A 1988 *Surf. Sci.* **195** 226
[9] Ganz E, Sattler K and Clarke J 1989 *Surf. Sci.* **219** 33
[10] Maurcie V and Marcus P 1992 *Surf. Sci.* **275** 65
[11] Hinnen C, Imbert F, Siffre J M and Marcus P 1994 *Appl. Surf. Sci.* **78** 219
[12] Endo T, Sunada T, Sumomogi T and Maeta H 2002 *Mater. Charact.* **48** 159
[13] Ma Q and Rosenberg R A 1997 *Surf. Sci.* **391** L1224
[14] Moullet I 1995 *Surf. Sci.* **331** 697
[15] Mo Y W 1993 *Phys. Rev.* B **48** 17233
[16] Francis G M, Kuipers L, Cleaver J R A and Palmer R E 1996 *J. Appl. Phys.* **79** 2942
[17] Stabel A, Eichhorst-Gerner K, Rabe J P and González-Elipe A R 1998 *Langmuir* **14** 7324
[18] McBride J D, Tassell B V, Jachmann R C and Beebe T P 2001 *J. Phys. Chem.* B **105** 3972
[19] Zhu Y J, Schnieders A, Alexander J D and Beede T P 2002 *Langmuir* **18** 5728
[20] Gates A D and Robins J L 1982 *Surf. Sci.* **116** 188
[21] Busse C, Langenkamp W, Polop C, Petersen A, Hansen H, Linke U, Feibelman P J and Michely T 2003 *Surf. Sci.* **539** L560
[22] Humbert A, Dayez M, Granjeaud S, Ricci P, Chapon C and Henry C R 1991 *J. Vac. Sci. Technol.* B **9** 804
[23] Anton R and Schneidereit I 1998 *Phys. Rev.* B **58** 13874
[24] Anton R and Kreutzer P 2000 *Phys. Rev.* B **61** 16077
[25] Bardotti L, Jensen P, Treilleux M, Hoareau A and Cabaud B 1995 *Phys. Rev. Lett.* **74** 4694
[26] Lewis L J, Jensen P, Combe N and Barrat J L 2000 *Phys. Rev.* B **61** 16084
[27] Goldby I M, Kuipers L, von Issendorff B and Palmer R E 1996 *Appl. Phys. Lett.* **69** 2819
[28] Bogicevic A, Strömquist J and Lundqvist B I 1998 *Phys. Rev. Lett.* **81** 637
[29] Stumpf R and Scheffler M 1994 *Phys. Rev. Lett.* **72** 254
[30] Stumpf R and Scheffler M 1996 *Phys. Rev.* B **53** 4958
[31] Donohue J 1974 *The Structures of the Elements* (New York: Wiley)
[32] Kushvaha S S, Yan Z, Xiao W and Wang X S 2006 *J. Phys.: Condens. Matter* **18** 3425
[33] Xiao W, Yan Z, Kushvaha S S, Xu M and Wang X S 2006 *Surf. Rev. Lett.* **13** 287